A SPATIALLY EXPLICIT INDIVIDUAL-BASED PLANT INVASION MODEL OF

CORTADERIA JUBATA

By

Ward B. Nickle

A Thesis
Presented to
The Faculty of Humboldt State University

In Partial Fulfillment
of the Requirements for the Degree
Master of Science

May 2008

A SPATIALLY EXPLICIT INDIVIDUAL-BASED PLANT INVASION MODEL OF
CORTADERIA JUBATA

HUMBOLDT STATE UNIVERSITY

By

Ward B. Nickle

Approved by the Master's Thesis Committee:

Dr. Kenneth Owens, Major Professor	Date

Dr. Mark Rizzardi, Committee Member	Date

Dr. Erik Jules, Committee Member	Date

Dr. Sharon Brown, Graduate Coordinator	Date

Chris A. Hopper, Interim Dean for Research and Graduate Studies	Date

ABSTRACT

A SPATIALLY EXPLICIT INDIVIDUAL-BASED PLANT INVASION MODEL OF

CORTADERIA JUBATA

Ward B. Nickle

It is the intent of this study to simulate the invasion of *Cortaderia jubata*, jubata grass, into a disturbed second growth redwood forest where the dynamics of the grass and its relationship to the environment are explored through a spatially explicit individual based landscape model. The field of neighborhood approach is used to simulate both the evolution of the forest and the grass. What is of particular interest is the success of the invader in terms of spatial distribution and time with regard to varying disturbance regimes. To assess these qualities, seed dispersal and the field of neighborhood each plant exerts are used to parameterize the model and a measurable plant attribute, self thinning, not included in the model assumptions, is used to test the model's validity.

TABLE OF CONTENTS

LIST OF FIGURES

1. INTRODUCTION AND BACKGROUND

Biological invasions of plants are ubiquitous and their study is invariably essential to the understanding of an ecosystem (Vitousek et al. 1996). There has been much concern in recent years in categorizing, and attempts to explain, causal factors contributing to the establishment, persistence, and rate of spread of invading organisms (Burke and Grime 1996, Drake et al. 1989). To a large degree, many of these causal factors have been shown to be overly broad (Lambrinos 2002, Higgins et al. 1996, Higgins and Richardson 1998a). It has been suggested that ecosystem specific characterizations are the best method to investigate plant invasions (Wu and Levin 1994).

Plant invasions often produce undesirable economic and environmental impacts by decreasing the abundance of agriculturally or ecologically valuable species (Drake et al. 1989, Higgins et al. 2000). As basal components of the landscape, plant invasions inherently alter ecosystems (Lambrinos 2001) making their establishment a cause for concern. A predictive understanding of plant invasions allows us to mitigate these realities (Higgins and Richardson 1998b).

Grasses are a group of invasive species that are important because grasses are frequently moved by humans making their invasion common, they are effective competitors, they are capable of altering ecosystem processes such as nutrient cycling, and by affecting local climate and fuel loads, grasses perpetuate fires (D'Antonio and Vitousek 1992). Additionally, grasses can hinder the establishment of seedlings in

coniferous forests (DiTomaso et al. 1999, Cowan 1976) which is of particular concern in this study.

Jubata grass has become a problem in many parts of the world. In the forests of New Zealand and Australia in particular, jubata grass has become an invasive pest (DiTomaso et al. 1999, Popay et al. 2003). Jubata grass has been widely planted in Hawaii where it is invading rain forest and alpine shrubland. There is an abundance of evidence which suggests some level of environmental disturbance is necessary in order for a plant invasion to occur. Accordingly, jubata grass is commonly found in deforested areas, eroded banks and hillsides, or otherwise disturbed areas (DiTomaso et al. 1999, Costas-Lippmann 1976). In this study we develop a spatially explicit individual based model to examine the rate at which, and to what extent, jubata grass (*Cortaderia jubata*) invades the managed coastal redwood (*Sequoia sempervirens*) forests of Northern California. It is the intent of this study to describe the local competition that plants face, both inter-specifically and intra-specifically, in the midst of invasion.

1.1   Jubata Biology

Jubata grass, a perennial grass with large plumes extending from a tussock base surrounded by long 3-5 ft. blades, was introduced to California as an ornamental from the Andean regions of Ecuador, Bolivia, and Peru, in the mid 1850's and was cultivated commercially by Joseph Sexton, near Santa Barbara, CA, who was exporting 500,000 plumes annually (Lambrinos 2000). By 1967, D. W. Cooper, a farm advisor, reported that 8,000 acres of cut-over redwood forest land had been invaded by jubata grass

(Cooper 1967). The species was lauded as palatable to cattle, and its planting was advocated. There are two species of jubata grass, *C. jubata* and *C. sellona*. The weedier of the two species *C. jubata*, also called pampas grass, is the variety present in the redwood forest. The plumes of jubata grass can produce 100,000 seeds each and large plants are capable of producing over 1,000,000 seeds (Cowan 1976). The seed of *C. jubata* has been shown to have a 0-4% germination rate (Costas-Lippmann 1976). Jubata grass, which can live up to 15 years (Pleasants and Whitehead 1977), prefers coastal settings as it can not tolerate drought, or extreme heat. Accordingly, 91% of California's jubata grass can be found on the foggy north coast (Lambrinos 2002). *C. jubata* is asexual ensuring reproduction among isolated populations and without the presence of pollinators, unlike the related species *C. sellona* (Lambrinos 2000). This attribute of *C. jubata* has been implicated in its success as an invader spreading through California at a rate of 107 km²/yr (Lambrinos 2002). Additionally, it has been demonstrated that the ability of jubata grass to expand from founding populations threatens native diversity (Lambrinos 2000).

1.2 Redwood Biology

Coast redwood is the world's tallest known tree and one of the longest lived, capable of measuring up to 360 feet tall and living upwards of 2000 years. Redwoods are monoecious evergreens endemic to the coastal areas of northern California and southern Oregon (Olson et al.1990). While redwood is a commercially valuable timber species (Metcalf 1924), it also provides habitat for many threatened or endangered animals

including the spotted owl and the marbled murrelet (Abate 1992). Redwoods have deep, lateral roots systems and thick fibrous bark. They regenerate through seed production and sprouting. At between 5 and 15 years of age redwoods begin to produce viable seed which have a low germination rate and a 200-400 ft dispersal distance (Olson et al. 1990). It has been shown that trees in excess of 250 years old produce the most viable seed (Metcalf 1924). Redwoods are also capable of reproducing asexually by sprouting from existing growth and it is the sprouts from root crowns that are preferred for generating new tree crops (Boe 1975).

1.3   Modeling Strategies

Many modeling strategies have been employed in the field of ecology. With regard to landscapes in specific, there have been three main types of modeling approaches: whole landscape models, distributional models, and more recently, spatially explicit models (Andow et al. 1990, Higgins and Richardson 1998a, Okubo 1980, Skellam 1951, Wu 1994). Whole landscape models, such as reaction-diffusion models, look at a landscape in its entirety by describing the collective value of a variable, such as the population size of a particular species, throughout the landscape. Distributional models are primarily concerned with examining how variables are distributed across various landscape elements, as in a heterogeneous setting. Spatially explicit models offer a finer level of detail in that they describe precise information of landscape attributes at specific locations.

Particular attention has been paid to the spatial scale of spatially explicit models. Many spatially explicit models use matrices as a spatial framework (Higgins and Richardson 1998b, Watkinson et al. 2000). Each element of the matrix corresponds to the value of the variable associated with the matrix. The position of the element within the matrix corresponds to the location of the spatial process being modeled, which is usually a rectangular region, or, cell. It has been shown that spatially explicit models' predictions are sensitive to the size of these cells and it has further been suggested that the spatial grain of the model should be compatible with the processes being modeled (Higgins et al. 1996). Spatially explicit models add an even finer grade of detail when each individual of interest within the landscape is modeled separately. This type of information intensive modeling has only become recently practical with advances in personal computers (Berger et al. 2002).

Spatially explicit individual-based models (SEIBMs), which are often built from the ground up, do not have well known properties and are usually quite complex, unlike well known standard models which have more general applications (Grimm 2002). However, it has been shown that spatial models place more emphasis on interactions between ecological processes than diffusion models (Higgins and Richardson 1998a) and are thus better suited for describing the ecology of biological invasions. We develop a SEIBM based on the methods presented by the Berger et al. (Berger and Hildebrandt 2000, Berger et al. 2002) in the creation of a single species mangrove forest model, KiWi.

2. METHODS

2.1   The Model

The spatially explicit individual-based model, in which time is considered in discrete annual increments, consists of two parts, a single species model and a two species model. First, the single species coast redwood (*Sequoia sempervirens*) model simulates an even aged, second growth forest in which to introduce the invading species, jubata grass (*Cortaderia jubata*). After the forest reaches 100 years old, 10% of the trees are harvested along one boundary, and a single jubata plant is introduced. This process is then repeated for various initial redwood densities [number of trees/hectare]. Both inter-specific and intra-specific competition are modeled according to the field of neighborhood approach (Berger and Hildebrandt 2000, Berger et al. 2002). The model was built using Matlab version 6.1 and regressions were calculated with Excel 2002. The model subroutines were executed in the order presented below.

2.2   The Forest

To simulate the redwood forest, a 1 hectare spatially homogeneous two dimensional landscape is considered. To discretize the space, only integer values of Cartesian coordinates in meters are considered as candidates for plant centers, and the landscape is bounded on all sides. The forest simulation is initialized with randomly distributed seedlings with 1 centimeter radii. The trees are then assigned an age of one

and their spatial distribution and age are stored. For every year that follows, the strength of the competition that each plant exerts on its neighbors is calculated according to the field of neighborhood approach which is then used to determine the growth rate for an individual. At the end of each year, every plant is aged and both the spatial distribution and age are stored. Figure 1 illustrates an overhead view of an initial redwood seedling distribution in which the green circles correspond to basal areas.

2.3   Field of Neighborhood

The field of neighborhood approach (Berger and Hildebrandt 2000, Berger et al. 2002) is a new modeling technique that elegantly captures many of the less tractable attributes of plant competition. This technique attempts to create a standard for the individual-based modeling of plant populations by integrating the zone of influence and ecological field approaches to model plant competition. Both of these techniques assume a circular region of influence, surrounding the base of each plant, in which competition for resources occurs. The circular region of influence is a function of the size of the plant which it surrounds. Within the context of the zone of influence approach, the competition a plant exerts is assumed to be constant throughout the region of influence, which is overly simplified. Alternatively, the ecological field approach assumes a spatially explicit field within the region of influence that describes in a complicated and little used manner how a plant modifies its environment (Berger et al. 2002).
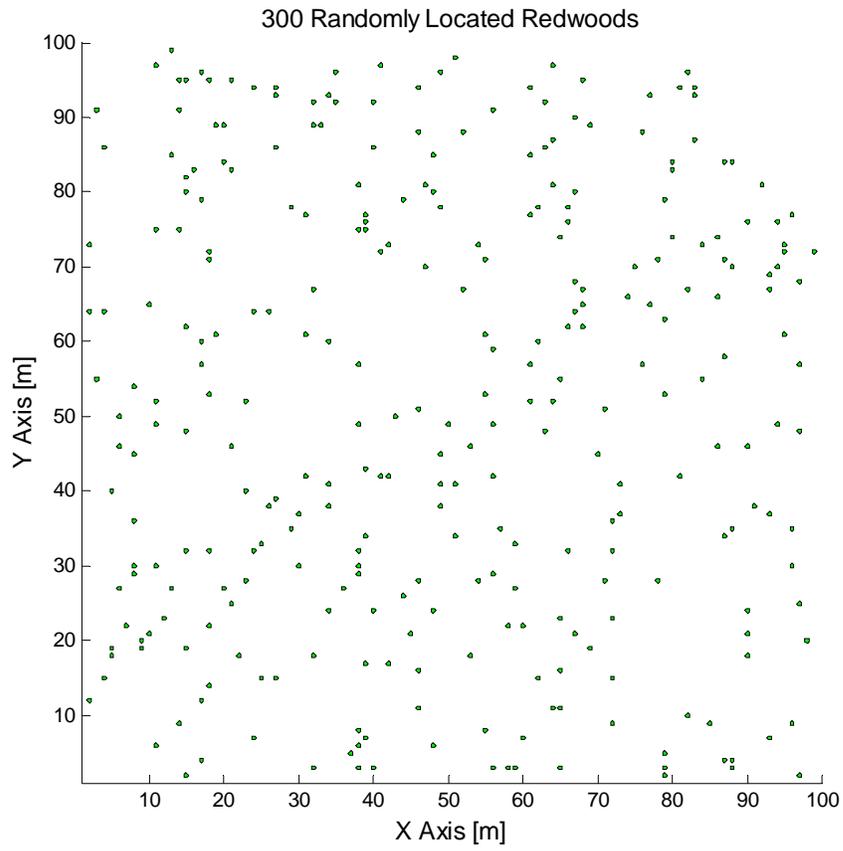
Figure 1.   Randomly generated redwood distribution. The landscape is a single, spatially homogeneous, hectare bounded on all sides.

The field of neighborhood approach streamlines these ideas by assuming an exponentially decreasing competition strength as one moves away from a plant's outer boundary. Berger et al. (Berger and Hildebrandt 2000, Berger et al. 2002) define this region of influence as the *field of neighborhood*.

The field of neighborhood, R, is defined by the function $R = a * r^b$, where r is the radius at breast height of the plant in meters, and a and b are parameters. As the parameter b increases, R decreases for values of $r < 1$, which can be seen in Figure 2. Additionally, as one can infer from the equation, the parameter a is a scale factor, allowing it to stretch or compress R. Radial carrying capacities are 150 cm and 350 cm for the jubata and redwood species respectively.
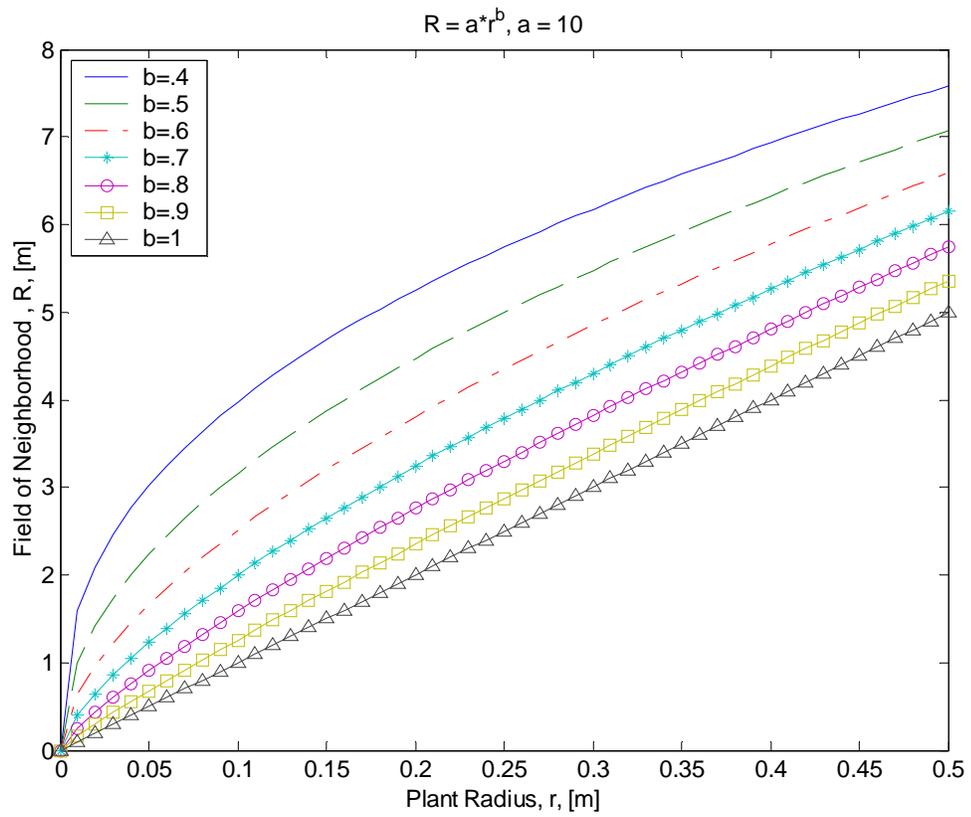
Figure 2.   Radius of the field of influence as it is affected by varying the parameter b. The value of parameter a is held constant at 10.

Competition strength is viewed as a number between 0.1 at the edge of a region of influence and 1 throughout the basal area of the stem. This region of influence is circular, centered about each plant, and of radius $r + R$, the radius of influence. Elsewhere the plant's influence is 0. This competition strength is exuded two dimensionally and is radially symmetric. For each point (x, y) in the landscape, the competition strength of all plants whose influence reaches that point, including the competition exerted by a plant located at (x, y), is calculated as follows

$$F(x, y) = \sum_{i,j} \begin{cases} 1 & ,0 \le d_{i,j} \le r(i, j) \\ .1^{\frac{d_{i,j}-r(i,j)}{R(i,j)}} & ,r(i, j) < d_{i,j} \le R(i, j) + r(i, j) \\ 0 & ,d_{i,j} > R(i, j) + r(i, j) \end{cases}$$

where

- $F(x, y)$ is the competition strength exerted by all plants on point (x, y)

- (i, j) is a plant location

- $d_{i,j}$ is the distance from (x, y) to the plant at (i, j)

- $r(i, j)$ is the radius of a plant located at (i, j)

- $R(i, j)$ is the field of neighborhood of the plant located at (i, j) and

- $r(i, j) + R(i, j)$ is the radius of influence of the plant located at (i, j) .

Figure 3 depicts the competition strength for a single redwood with a radius of .43 meters, the radius of a redwood that is approximately 120 years old within the context of this model. In the graph, the sign of the x axis indicates direction and the field of neighborhood parameters a and b are 10 and 0.7 respectively. We can see that these values of the parameters and the radius of the tree yield a field of neighborhood of 5.53 meters.

In Figure 3, space is only considered one dimensionally as competition strength is the vertical axis. The model itself is two dimensional and is discretized for integer meter values of the landscape. So, Figure 4 depicts the discretized competition in two dimensions.
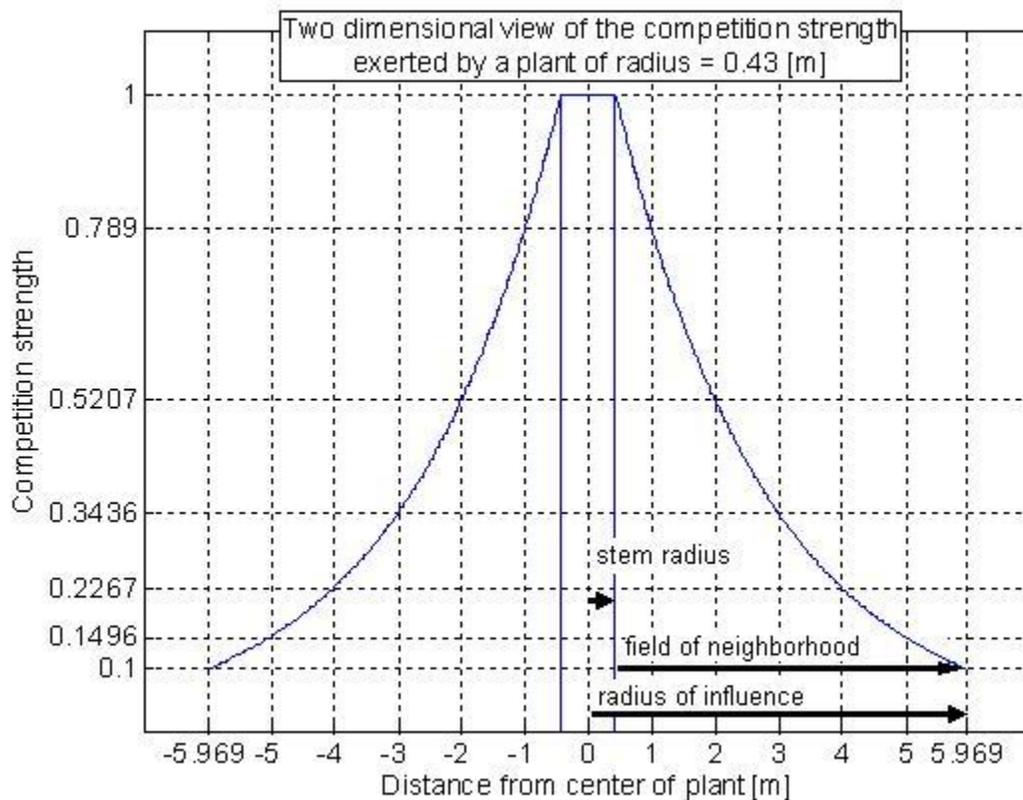
Figure 3.   Competition strength as a function of distance from the stem center. This
    strength is 1 inside the basal area of the stem, exponentially decreases as one moves
    away from the stem, and is 0 outside the field of neighborhood.
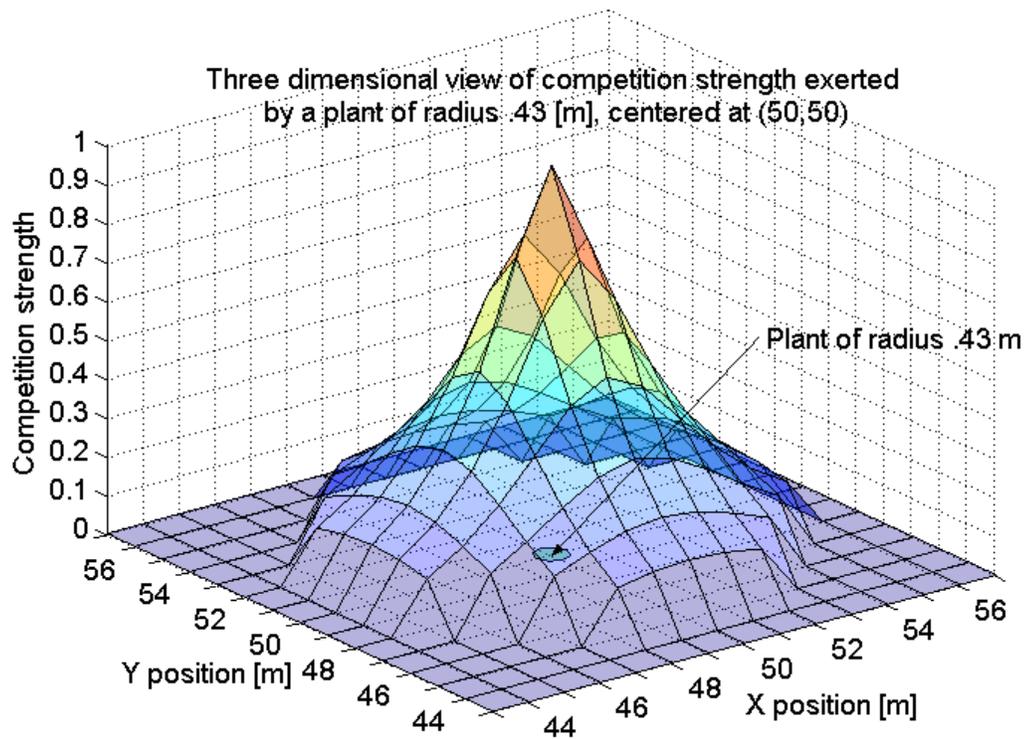
Figure 4.   Graph of the competition strength exerted by a single plant. The landscape is discretized for integer meter values and the competition strength is exuded in a radially symmetric, exponentially decreasing, manner.

This competition strength is normalized by considering how much competition each plant is experiencing per square meter of its region of influence. This is achieved by summing the entire competition in each plant's region of influence, subtracting its self-competition, i.e., the competition added to the region by the plant itself, and then dividing by the total area within the region of influence. So for a plant centered at (x, y), the normalized competition it experiences can be represented by

$$F_A(x, y) = \sum_{i,j}\{[F(i, j) - F_{self}(i, j)]/A\} \ \forall \ (i, j) \in FON(x, y)$$

where

- $F_A(x, y)$ is the normalized competition strength experienced by the plant located at (x, y)

- $F(i, j)$ is the competition strength exerted by all plants on point (i, j)

- $F_{self}(i, j)$ is the competition strength contributed to point (i, j) by the plant located at (x, y)

- A is the area in square meters of the region of influence of the plant located at (x, y)

- $FON(x, y)$ is the set of points (i, j) in the field of neighborhood of the plant located at (x, y).

In biological terms, F_A is a measure of how much a plant is competing for nutrients, light and water per square meter of its region of influence. So, for a plant experiencing no competition from any neighbor, $F_A(i, j) = 0$. This normalized competition strength is used in determining growth, which is discussed in Section 2.6 .

<div align="center">2.4   Optimal Radial Growth Curve</div>

An important assumption of the model is the estimation and application of optimal radial growth curves. These aspects of the model, along with the parameters a and b, which determine the field of neighborhood, are of significant importance. The parameterization of the growth curve, as well as the species specific parameters a and b, are the primary qualities of the model that dictate how plants grow and compete. Age structured data used for parameter estimation of growth curves is nearly non-existent for the two species examined here.

Though data certainly exists, little data explicitly describes the radial growth of a species as a function of time. These types of longitudinal studies are impractical for many plant species, especially long-lived species like redwoods. Typically, sigmoidal curves are estimated to approximate plant growth as a function of time. To our knowledge, the best available data to predict optimal growth curves for redwood trees is the so-called Wonder Plot data. This plot, which is near Fort Bragg, California, originally consisted of 259 second growth redwood trees and was established in 1858. Tree radii were was first measured on this plot by Emanuel Fritz in 1923 and measurements were repeated every 10 years until 1995 (Allen, et al. 1996). The stand

serves as "an interesting case study in the growth and yield of second growth redwood on

the highest [quality] of sites," as stated by Allen et al. (1996) in their analysis of the 72

years of data. We took the data and removed any discrepancies in terms of trees that

were not consistently re-measured larger than they were ten years prior. Additionally, we

removed any trees that had died because they were not optimal plants to consider. The

data, biased for optimality, then consisted of 90 trees with 8 measurements each.

Minimum and maximum data was also added which described a plant with 0 radius at

year 0 and 350 cm radius at year 2200 (Brown 1996). This data was then averaged and

the curve displayed in Figure 5 was fit to the data where r is the tree radius in centimeters

and t is time in annual increments. We attempted to fit a logistic curve to the data

because growth curves are generally sigmoidal implying they have some limit to growth.

This is obviously due to some physically limiting factors that prevent infinite growth.

However, for our data the logistic fit produced unsatisfactory results. This is primarily

because the data has a linear trend for small values of t, which is inconsistent with the

exponential growth assumed by logistic functions. However, if the trees lived to 2000

years the sizes predicted by a linear function would be unreasonable. So, we decided to

use a model of the form

$$\frac{dr}{dt} = k\left(1 - \frac{r}{r_{max}}\right).$$

This model assumes that the change in radius is linear for small values of r and slows as

r approaches r_{max}. The solution to the above equation was found to be

$$r(t) = r_{max} - (r_{max} - r_0)e^{(-kt/r_{max})}.$$

Using linear regression we were able to fit the data to an equation of this form, which

proved to be the most satisfactory for both species examined (see Figures 5 and 6).

While certain data exists for the jubata grass, the only data we were able to find

that specifically related radial growth to time was from a North Carolina State University

floriculture study that focused on herbicide comparisons (Whipker et al. 2007). The

study provided a greenhouse grown control group for which optimal conditions were

provided. The data consisted of three diameter measurements taken at 5, 16, and 24

weeks of growth. In the absence of a more preferable, longitudinal, data set, we added

another data point for the estimated maximum age and size of a jubata plant, 15 years and

a 150 centimeter radius (Popay et al. 2003). We attempted several types of functions to

fit the data and found the best result was the growth equation we used for the trees since

the jubata grass exhibited a similar linear data trend for values of r less than r_{max}.

2.5   Initialization

The single species redwood model is initialized with a varying amount of

randomly dispersed year old saplings. For each initial density of trees, the model allows

the forest to grow and compete with itself, i.e., intra-specific competition. After 100

years of growth and self thinning, 10 percent of the forest biomass (Jenkins et al. 2003) is

harvested along a single boundary. This essentially clear cuts an edge of the forest

thereby creating disturbance and a gap. A single jubata grass clump is introduced to this

region of the forest and the model is run for an additional 20 years.

$$r(t) = 350 - (350 - 0.734) * e^{(-0.385t/350)}$$
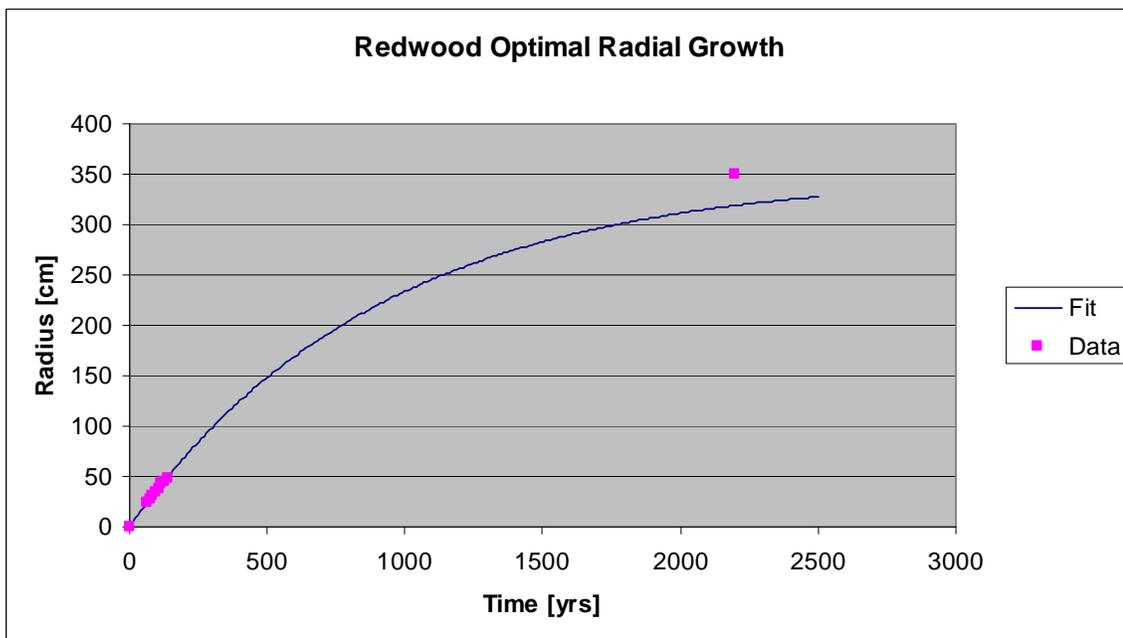
Figure 5.　The radial growth curve for coast redwood under optimal growing conditions. The curve was fit to the Wonder Plot Data (Allen et al. 1996) and minimum and maximum values.

$$r(t) = 150 - (150 - 6.227) * e^{(-194.085t/150)}$$
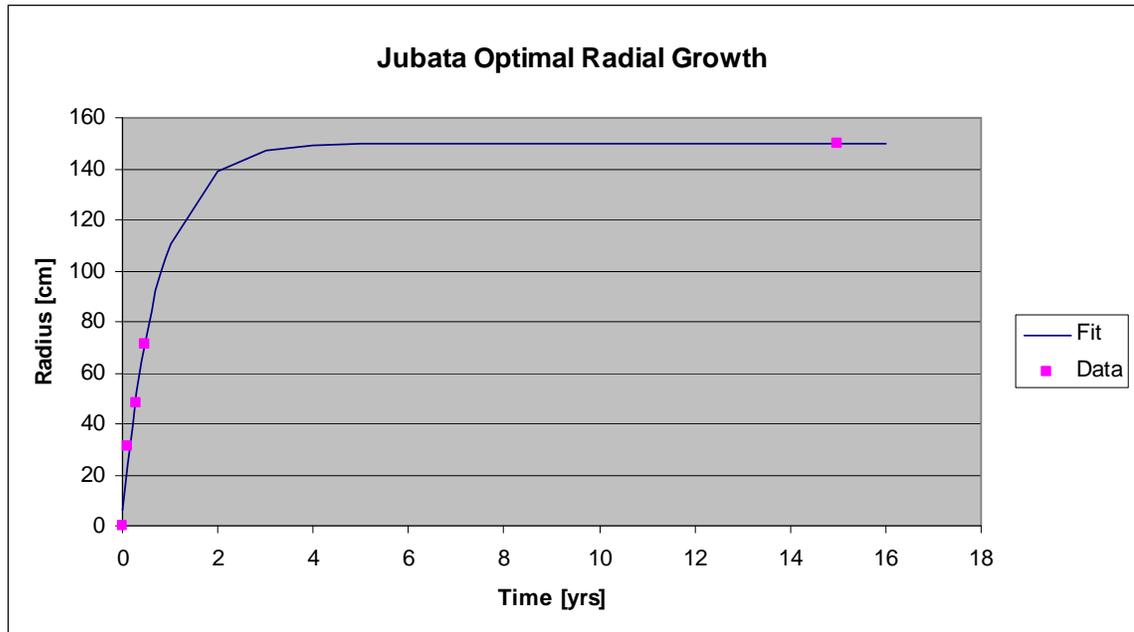
Figure 6.   The predicted optimal radial growth of C. Jubata based on the NCSU data (Whipker et al. 2007) and minimum and maximum values. The fit is used to predict the radial growth of an optimal plant.

2.6   Radial Growth

In each year of the simulation, radial growth is calculated according to a scaling of optimal growth (Berger at al. 2002). The optimal radial growth increment is the slope of the curve found in Section 2.5 which describes the total radius of a plant growing under optimal conditions as a function of time. Given an annual time step, the slope of the curve is approximately the difference of the two corresponding radial values.

The normalized competition a plant encounters from its neighbors, F_A, is used to scale the optimal growth increment. Since size is more likely to influence growth rather than age, the growth process begins by asking, "How long would an optimal plant have grown to reach the size of the given plant?" This time value is calculated from the radius of the plant in question using the inverse of the curve for optimal plants. Using this age, we can then find the optimal annual radial increment for a plant of the given size from the original curve.

If the competition strength is too high, i.e., $F_A \geq C$, where $C < 1$ is a competition threshold parameter, the growth scale factor is zero and thus the plant does not grow. Otherwise, the growth scale factor is $1 - F_A$. To illustrate this idea, assume $C = .5$, the optimal annual radial growth increment is 2 cm, and $F_A = .3$. Then the scale factor would be .7 and the plant's radius would grow 1.4 cm during that simulation year. Accordingly, growth decreases with increasing competition strength, F_A.

2.7   Memory

In order to overcome the challenge of simulating a death process for a botanical

species for which longevity data is scarce, a memory function is used according to Berger

and Hildebrandt (2000). Since a plant is likely to survive at least for awhile in the face of

competition, which is especially true in the case of higher plants such as trees (Berger and

Hildebrandt 2000), death occurs only when a plant does not grow optimally over a period

of T years. This allows for a few years of poor or no growth with the opportunity for a

plant to rebound if local conditions change. Thus, if the average competition strength

experienced per unit area, F_A, by the plant located at (i, j), over the last T years is more

than C, the plant has not grown to an optimal size. Consequently, if

$$\sum_{t=1}^{T} F_A(i, j)/T \geq C$$

then the plant located at (i, j) dies. The value of T is species specific. For the redwood

we chose $T = 5$, the memory allocated to a mangrove tree in the KiWi model. It was

assumed that the grass may not be able to tolerate as many poor years of growth as a tree

so for the jubata grass we chose $T = 2$.

With these values of T, the memory function behaved satisfactorily for the

redwood single species model but when the grass was introduced, the model exhibited

oscillatory patterns of over-saturation and subsequent death. In order to offset this

oscillation we introduced a random term to allow for the chance of death if a plant had

not grown to an optimal size in T years. In this manner not all the plants that experienced

inhibited growth for the same number of years would die simultaneously. So, if the

above mentioned conditions for death were satisfied, then the plant would die with

probability P, a user defined parameter. This random term was added to both species.

Adding this term created a more realistic model of self competition among the jubata

grass. Additionally, the jubata grass was allowed to die randomly with a chance of 5

percent annually to account for stochastic events such as herbivory.

2.8   Jubata Seed Dispersal

While both species considered here produce seed, we modeled only the seed of

the jubata grass as it is more viable, prolific, and it is well known that jubata grass out

competes conifer seedlings (Cowan 1976). Additionally, the 20 year invasion simulation

considered here is very small relative to a redwood's potential lifespan. Particularly, we

were interested in how an existing forest would interact within the context of disturbance

and the invasion of an alien grass. For the jubata grass, three different size regimes

(small, medium, and large) were established according to radius. For each size regime,

we modeled 20, 100, and 200 viable seeds respectively, representing 10%, 50%, and

100% of the maximum number of viable seeds. We chose these values by assuming that

2% of the up to 1,000,000 seeds are viable (Costas-Lippmann 1976). For these 20,000

seeds, we assumed a certain percentage survival. After parameterization we chose this

value to be 1%. Each seed was assigned a random angular direction according to a

uniform distribution. The probability density function, $d = -10 * \ln(U)$, in which U is a

uniformly chosen random variable, is used to model dispersal distance, describing a negative exponential distribution (Higgins and Richardson 1998b). The histogram in Figure 7 illustrates this model.

2.9   Jubata Seedling Recruitment

The jubata grass seedling recruitment is modeled by assessing whether a few simple criteria are met. If there is at least one viable seed, a gap, and a low enough competition for resources, then the seedling has a given probability of survival. Examination of these qualities makes sense in the ecological context of the model in that a seedling is unlikely to grow in the face of high competition for resources, a lack of space, or without a germinable seed. It has been argued that individual based models, which are often built from the ground up with complex results, are difficult to analyze and generalize (Grimm 1999). We utilize a method of "visual debugging", by creating animations of state variables, to develop and analyze the model, including the parameterization of the seedling recruitment phase of model simulation.
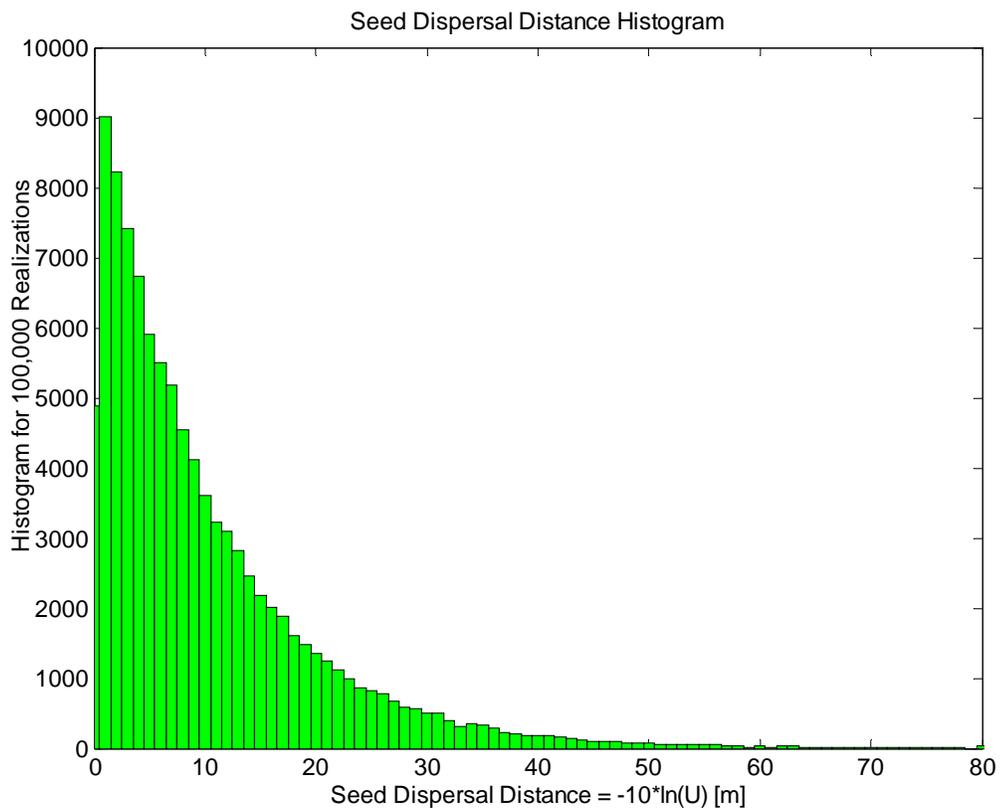
Figure 7.   The histogram represents the jubata seed dispersal distance. The graph was created by generating 100,000 uniformly distributed numbers and evaluating the dispersal distance.

3.   RESULTS

3.1   Self Thinning

To begin to verify the modeling process, we were interested if our model produced the characteristic self thinning observed in nature and other individual based models that implement the field of neighborhood description of local competition. Berger and Hildebrandt (2000) have shown that the self thinning induced by local competition creates realistic dynamics for the entire stand. Within the context of the single species redwood model, we tracked the biomass density trajectories for various values of competition strength as presented by Berger et al. (2002). This description is useful in that it shows the number of surviving trees and their average biomass [kg / individual] over the course of the development of the population. Biomass was calculated according to Jenkins et al. (2003).

The biomass density trajectories shown in Figure 8 reveal that by increasing the field of neighborhood parameter b, the trees are able to reach their maximum mean biomass more quickly, meaning essentially that the trees get bigger faster. Also, the trees are able to maintain higher densities as b increases. However, since the maximum mean biomass is determined by growth parameters and not competition parameters, it is the same for all values of b, about 3000 kg per individual. These results confirm the ability of our model to create realistic stand dynamics.
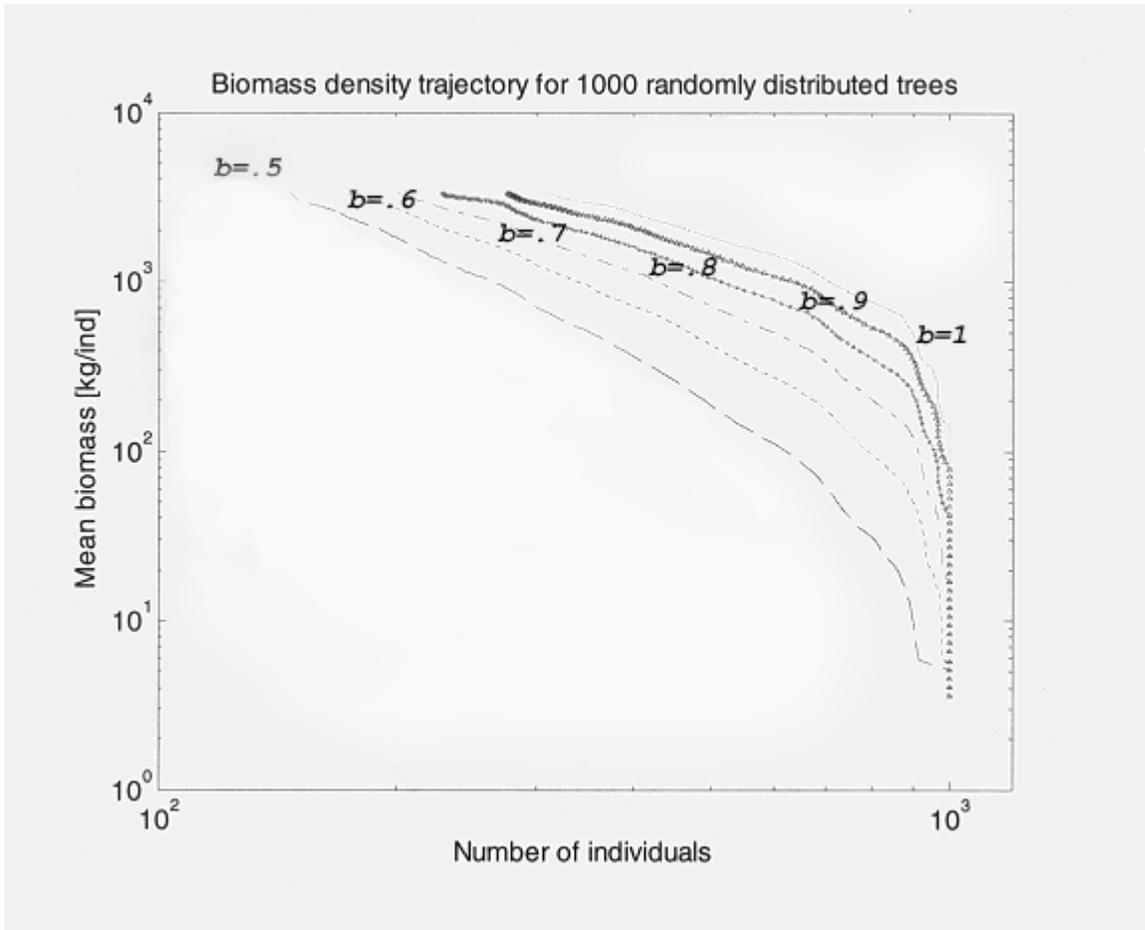
Figure 8.   The biomass density trajectory for various values of the field of
neighborhood parameter b. The results are the average of 50 simulations for each
value of b. Time passes as one reads the graph from right to left.

Additionally, we sought other descriptions of the model output. As most individual based models are built from the ground up, there is a lack of standards that can be widely applied with well known properties that are simple and easily generalizable, unlike classic theoretical ecology models (Berger et al. 2002, Grimm 1999). One approach involves using graphical representations of the model's state variables in combination with a graphical user interface, which could be downloadable and peer reviewed. This technique allows for debugging via performing controlled experiments to test and analyze the model throughout development and analysis (Grimm 2002). This sort of "visual debugging" was our primary method for parameter estimation as well as output analysis. While we could generate lists of data and relevant statistics about various characteristics of the model output, it seemed more illuminating to convey the spatial, temporal, and hierarchical characteristics of the model output simultaneously.

To examine these attributes of the competing plant species, we created animations to visually inspect the dynamics of parameter choices as well as to test the validity of the model.

3.2 Landscape Evolution

We built animations based on annual overhead snapshots of the landscape. In this manner we were able to see the plant populations develop and compete. With respect to the jubata grass species in particular, we were also able to view the effects of the seed dispersal and recruitment phases of plant development. Additionally, we were able to parameterize the model in such a way that the results were examined on a single species

basis, and once these parameters were chosen, the two species were combined. To illustrate these ideas we have chosen representative frames of the animations to convey their nature. Figures 9 -12 capture the forest under various stages of invasion beginning with the initial 10 percent disturbance along the southern boundary and the introduction of a single jubata plant. Since the possibilities of what to display are endless, we chose to include a representation from the middle of our range of initial tree densities, 153 trees per hectare.

The landscape view is informative for its spatial component while it has the added benefit of providing a temporal view as an animation. We were able to watch the landscape evolve and to examine local competition. We watched the spatial and radial attributes of the trees and grass "grow". This view gave us a feel for what the actual landscape might have looked like and it provided an adequate means of parameterizing the competition strength for each species. However, it did not show us what the plants themselves were experiencing in terms of competition for resources aside from inhibited growth produced by increased competition, or, conversely, uninhibited growth in the face of little or no competition. Therefore, we sought another way of visually exploring the competition plants experienced, or competition strength, as the landscape evolved.
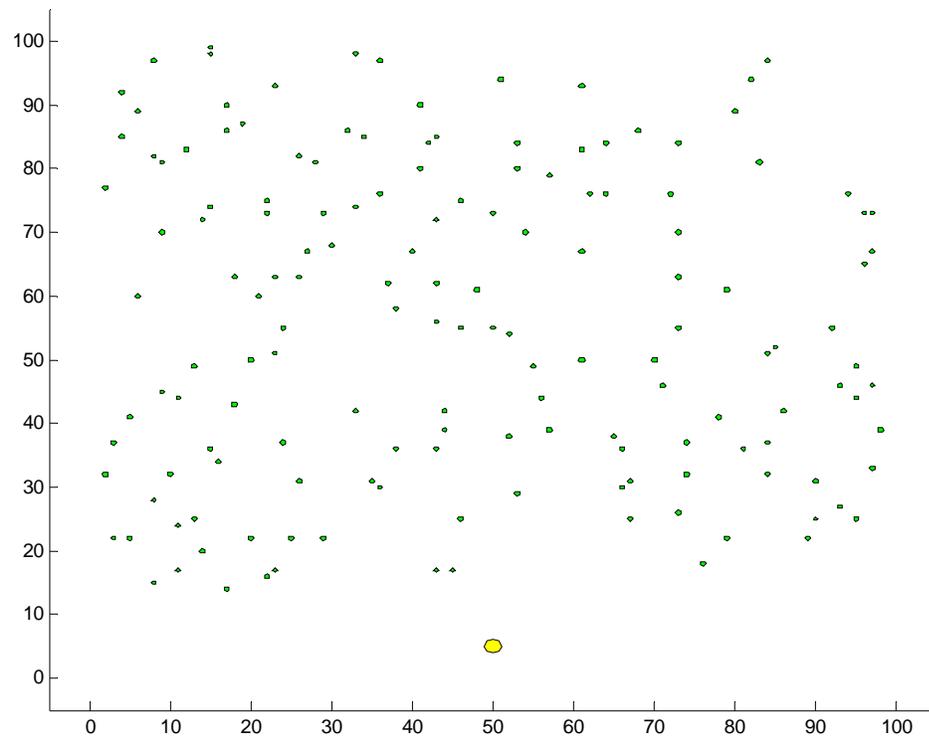
Figure 9.   An aerial view of the hectare forest. After 10 percent of the biomass is removed, an invasion front is created along the southern boundary. A single jubata plant is initialized in the center of this front.
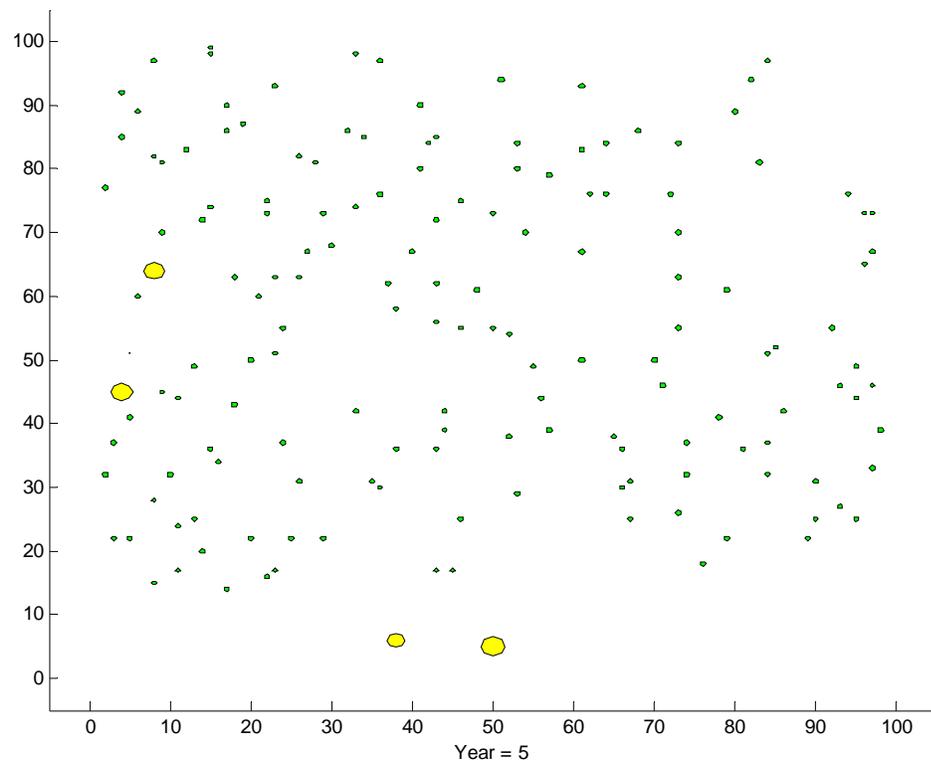
Figure 10.   The forest after 5 years of invasion. The dynamics of the seedlings are more clearly illustrated at higher resolutions. However, we can see the jubata grass population expanding into a gap in the forest floor.
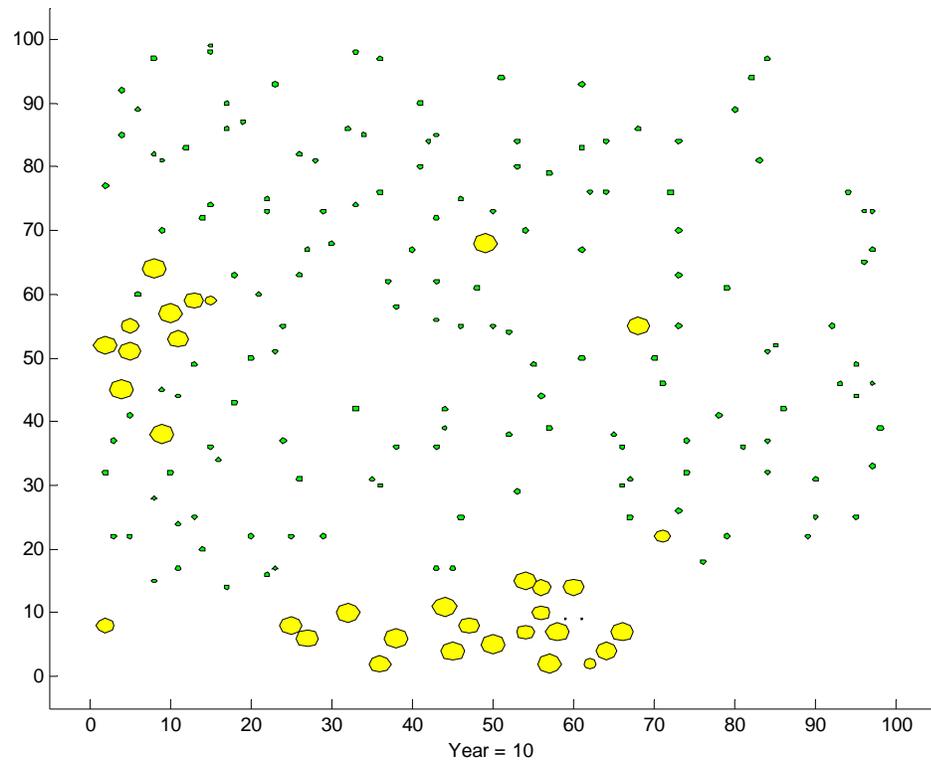
Figure 11.   After 10 years the jubata grass population has expanded significantly in both
range and number with founding populations spread across the southwest corner.
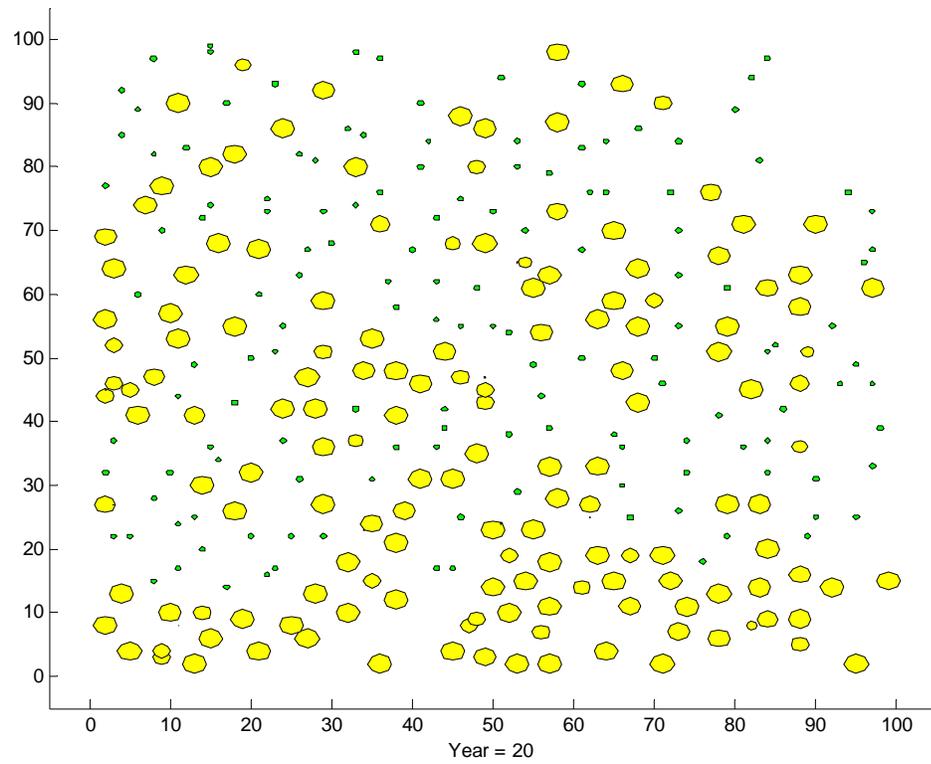
Figure 12.   After 20 years the jubata grass has infiltrated the entire forest. Some plants dominate the landscape and provide an ample source of seed.

3.3   Competition Strength

In order to visually describe the evolution of the competition for resources across the landscape, we stored the competition strength, F, and the normalized competition strength, F_A, at every point in the landscape, for every year during the invasion simulation. Similar to the results of Section 3.2, we represent the animation with a few important frames in Figures 13-16: when the invasion begins, and, 5, 10, and 20 years after the introduction of the alien grass.

These visualizations were very useful in describing total competition strength. Although, when the landscape becomes very crowded, this description is only good with the enhanced resolution offered by a graph that can be zoomed in on, turned, and rescaled. To accommodate these concerns for static graphs, like those imbedded, frame by frame, into our animations, we also visualized the normalized competition strength experienced per individual, F_A. This allows us to see on a plant by plant basis a value that is not only associated with local competition, but also with the size of the competing plant.

These images, shown in Figures 17-20, of the normalized plant competition convey values of F_A that are directly related to both the radial growth and death processes. This description is obviously relevant in the parameterization of the model by providing a landscape-wide view of an individual trait over time.
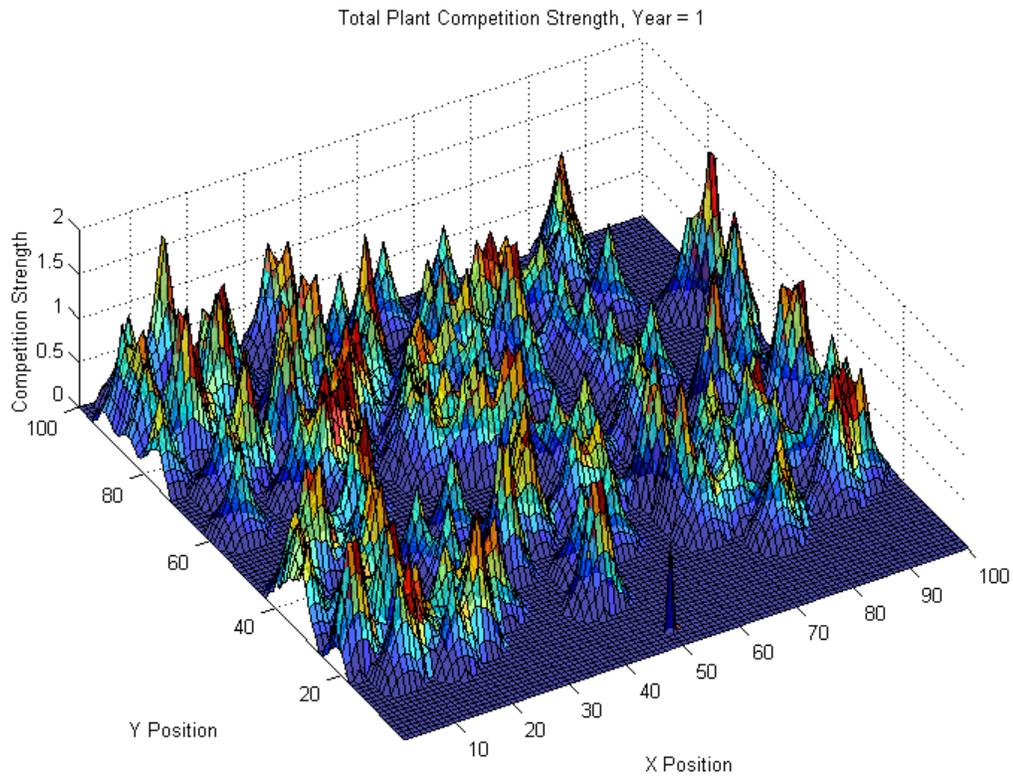
Figure 13.   Total competition strength for the entire landscape. This is the first year of invasion and the single jubata plant is established in the center of the invasion front, along the x axis.
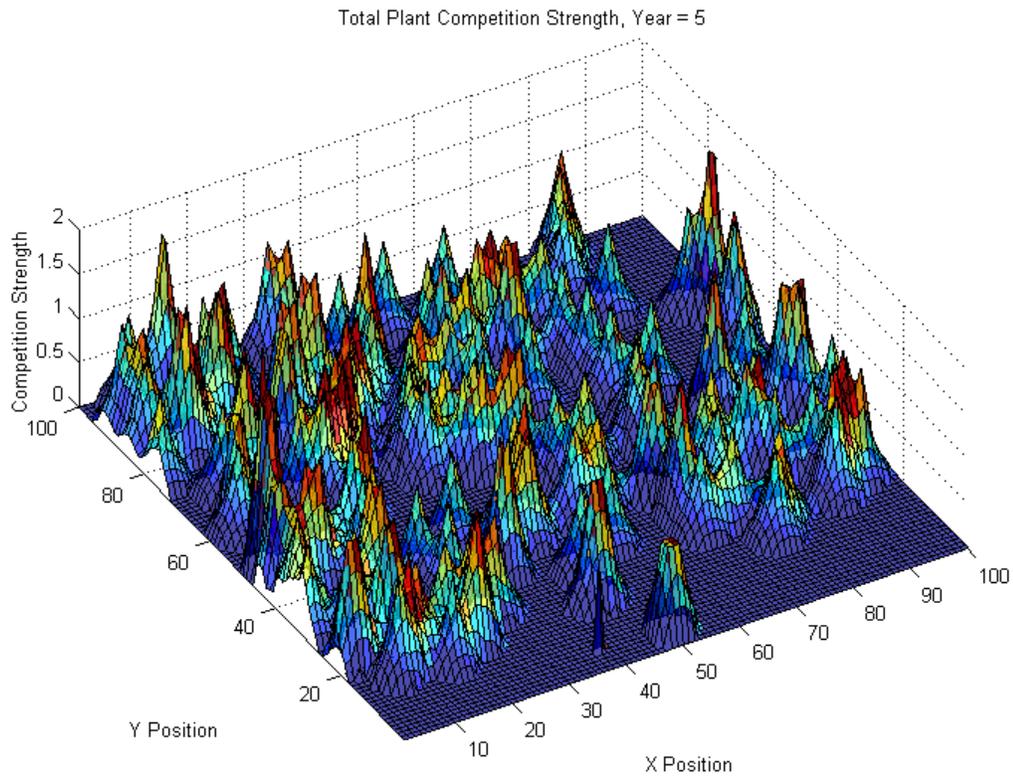
Figure 14.   The total landscape competition for resources at year 5. The jubata plant along the invasion front is exerting a much larger field of neighborhood. Additionally, a few more jubata plants have begun to compete within the undisturbed region of the forest.
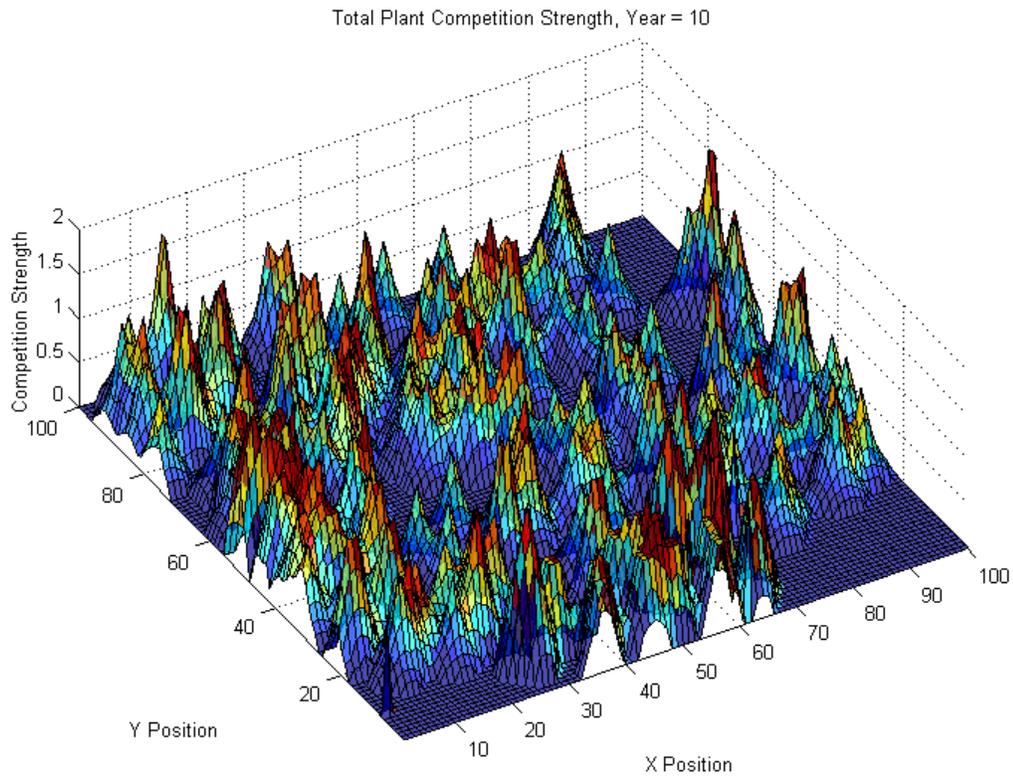
Figure 15.   The total competition across the landscape at year 10. The jubata population is making significant gains into the forest and the result is increased competition for resources as evidenced by peaks taller than 1.
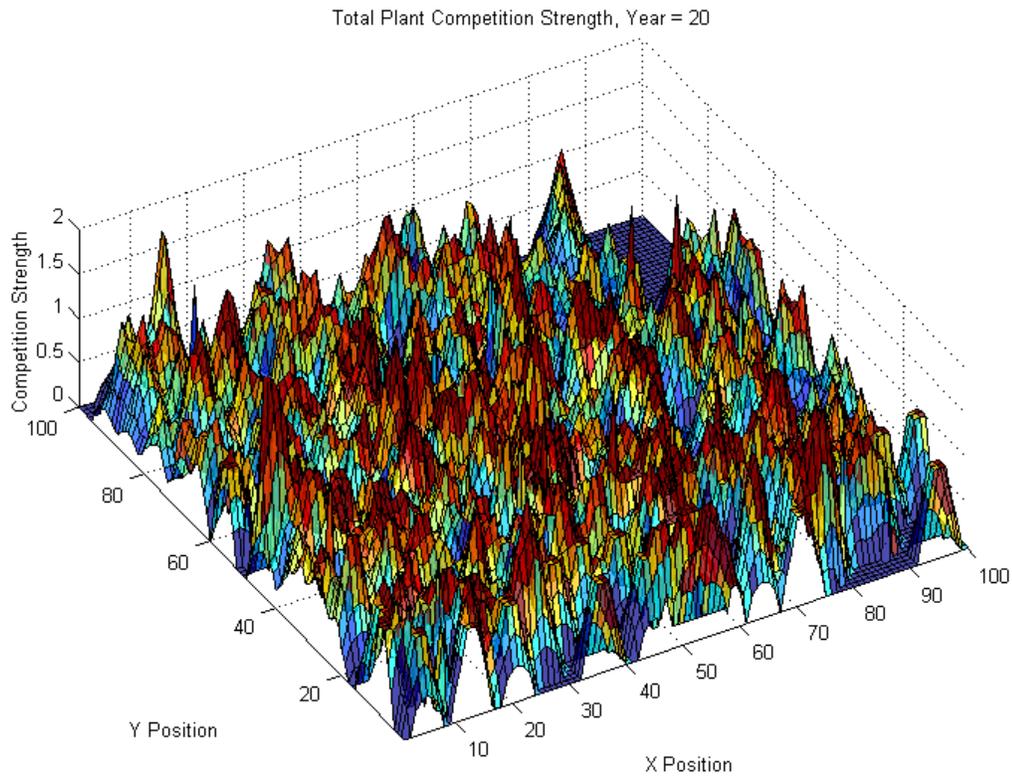
Figure 16.   Total competition for resources at year 20. The competition is fierce with nearly the entire surface of the forest floor now supplying resources for one or both species.
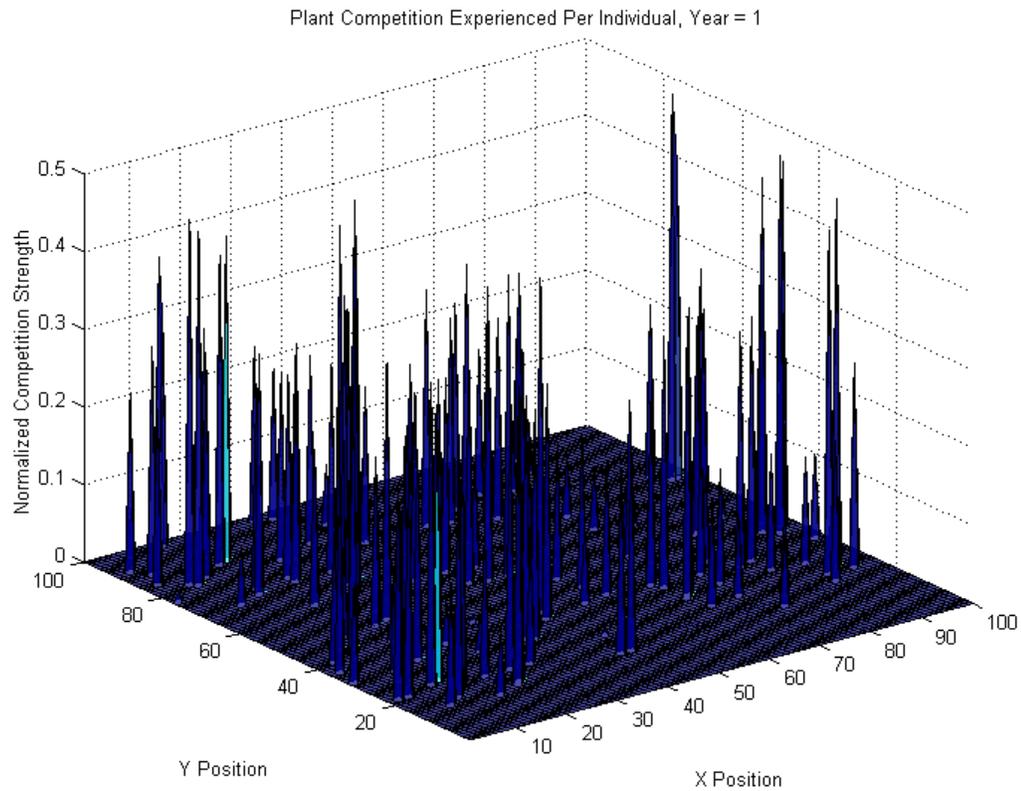
Figure 17.   Normalized plant competition at year 1. Many plants are well below the threshold for growth, $F_A = 0.5$. A plant experiencing a value of normalized competition greater than or equal to this threshold does not grow during the annual time step. If local conditions do not change over time, this sort of inhibited growth leads to plant mortality.
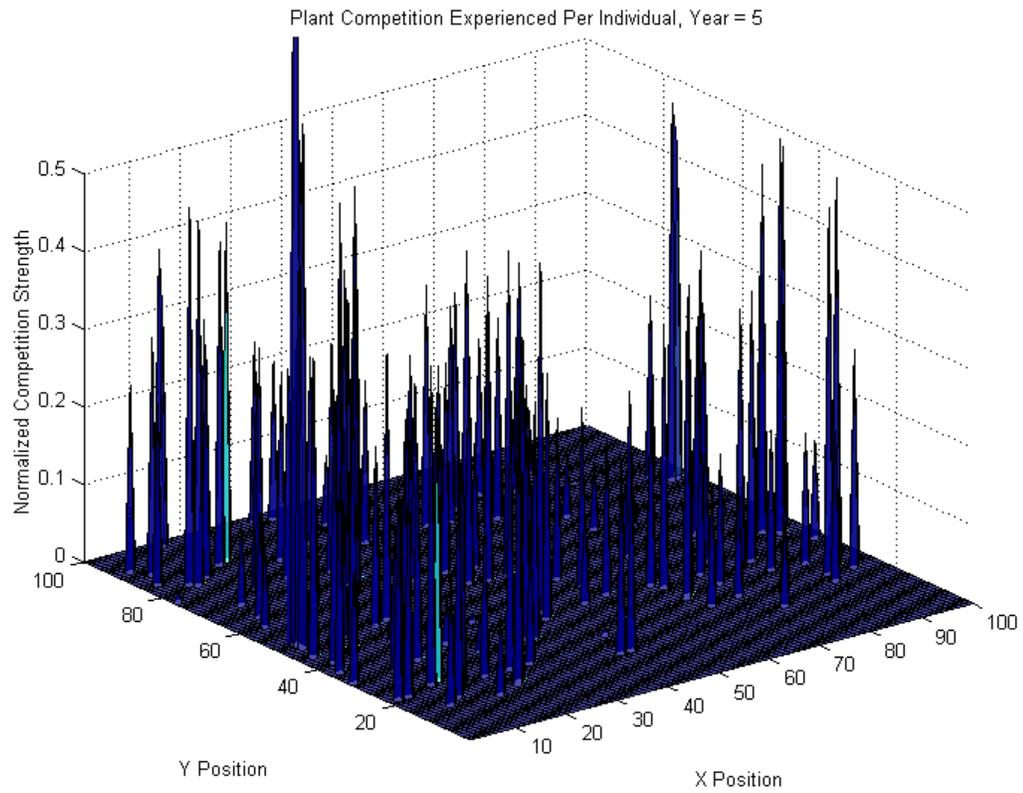
Figure 18.   Normalized plant competition at year 5. The competition within the forest is rising slightly with the establishment of a few more jubata plants.
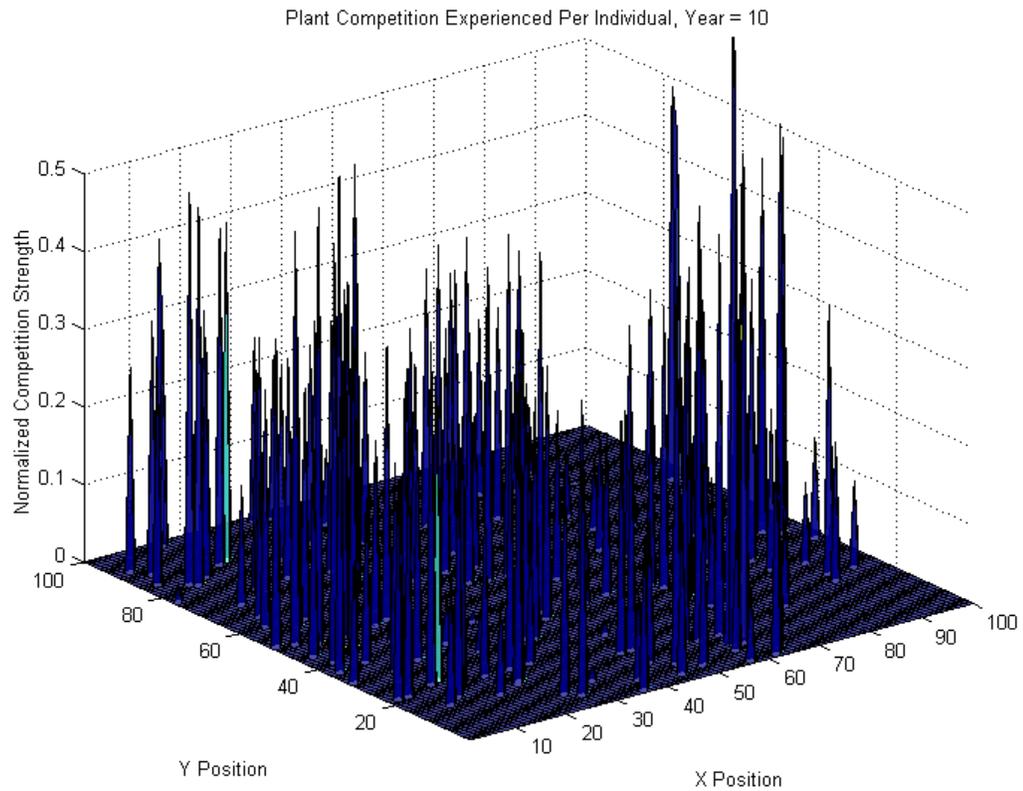
Figure 19.   Normalized plant competition at year 10. We see many plants now occupy the invasion front which introduces heightened competition in this region. Elsewhere, the normalized competition strength is increased by the introduction of more jubata grass throughout the forest.
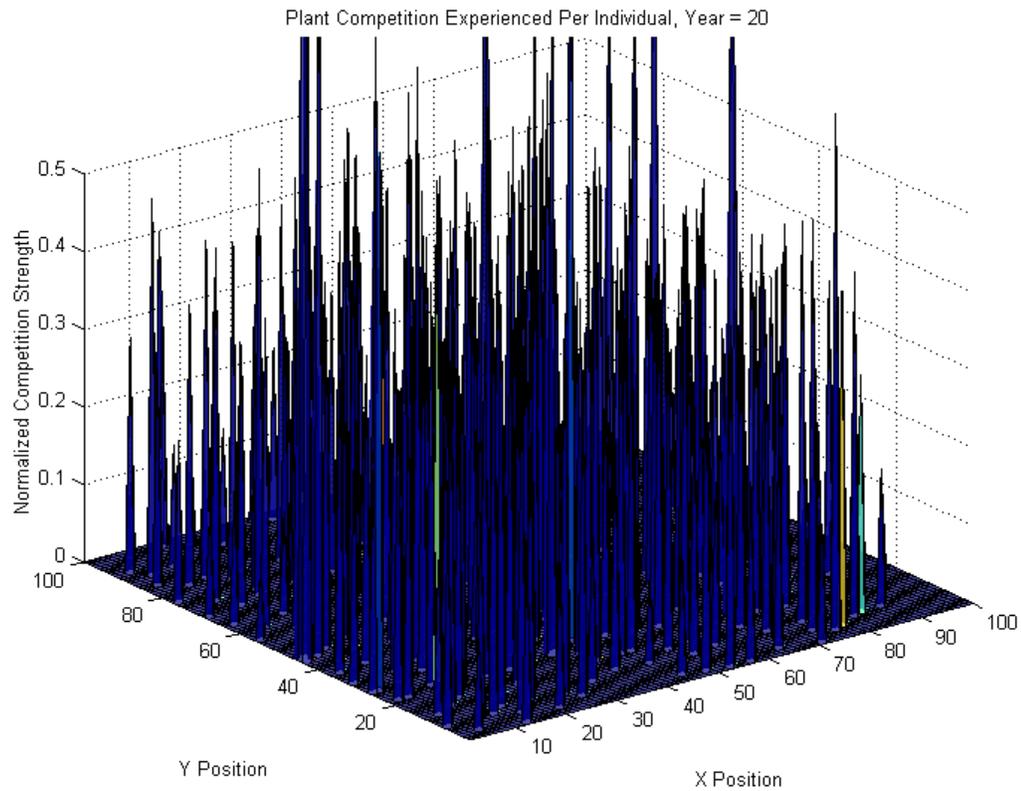
Figure 20. Normalized plant competition at year 20. By year 20 individuals are competing more intensely with the jubata grass taking hold of the forest floor. If these values of F_A are sustained, they are high enough to create death for many plants.

3.4   Management Tools

After parameterizing the model using the previously stated approaches to visual debugging, we wanted a meaningful way to capture the model's output in a way that would be useful to forest managers. We wanted to know what types of questions a forest manager would be concerned with. To this end we are very grateful to Dr. Christopher Edgar, in the Department of Forestry and Watershed at Humboldt State University. We reached the conclusion that an insightful characterization of the model's output could be achieved by plotting a 2 dimensional graph of the percent coverage of the jubata grass as it varied for different initial tree densities, for a particular moment in time. We then decided to extend this idea by asking what this graph would look like over the entire invasion simulation. So, we ran the model for 120 years for 40 different initial tree densities ranging from 10 to 400 trees per hectare, constituting 4800 years of simulation. During the first 100 years of each simulation, the forest self competed, which was followed by a complete 10 percent disturbance along the southern boundary, the initialization of a single invading jubata plant, and subsequently, 20 years of invasion. Figure 21 depicts the results of these model runs.
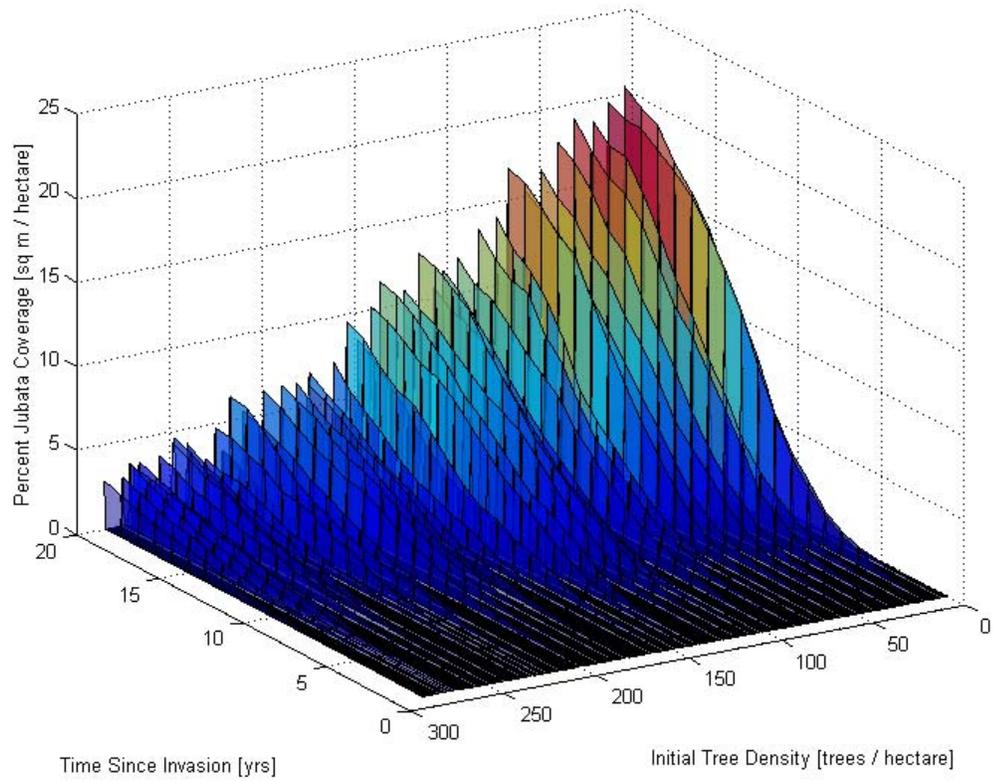
Figure 21.   The results of 40 invasion simulations for various initial densities. The tree densities reported represent the number of trees after disturbance, just before invasion.

This single result captures many of the model's layers of description at once. We can see that for low initial tree densities, the grass invades the landscape to a greater extent and more quickly, which can be seen by following the rightmost curves of Figure 21. The rate of change of invasion is evidenced by the increased slope for lower densities. It is clear that the establishment of jubata grass is inhibited by tree density. Lastly, we extended this information to account for all initial densities by interpolating between each slice of what could be viewed as surface, Figure 22.

The interpolated surface clearly conveys what we sought to establish with the previous representation. The timely establishment of jubata grass is largely suppressed by higher initial densities of trees. Additionally, the rate of jubata expansion is curtailed by these higher densities. To conclude our results we represent our interpolated surface with a contour plot, Figure 23.

This result is similar to the surface, however, the contours provide a view of different phases of invasion in an elegant and simple way. Here there are 6 clearly delineated phases of invasion that stretch across multiple layers of description. This representation seems more suited to the type of analysis and decision making that foresters might encounter. The graph indicates that, for higher densities of trees, a successful invasion could be staved off for a period of years, even when the grass is present. Further, the abundance of grass can be linked temporally to the relative age of the invasion with implications for decision making.

Figure 22.   The interpolated surface reveals the predicted values for any initial tree
     density.
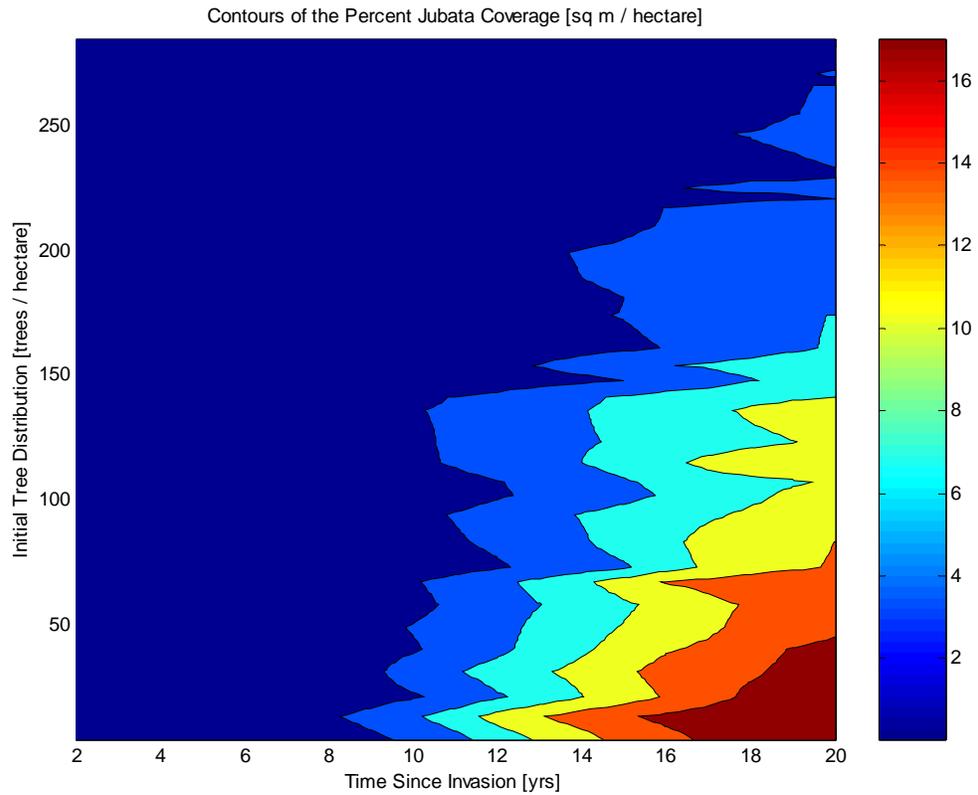
Figure 23. The contours of percent coverage jubata grass. We can see six distinct phases of invasion with the periods of increased jubata grass coverage only slightly affecting higher initial tree distributions.
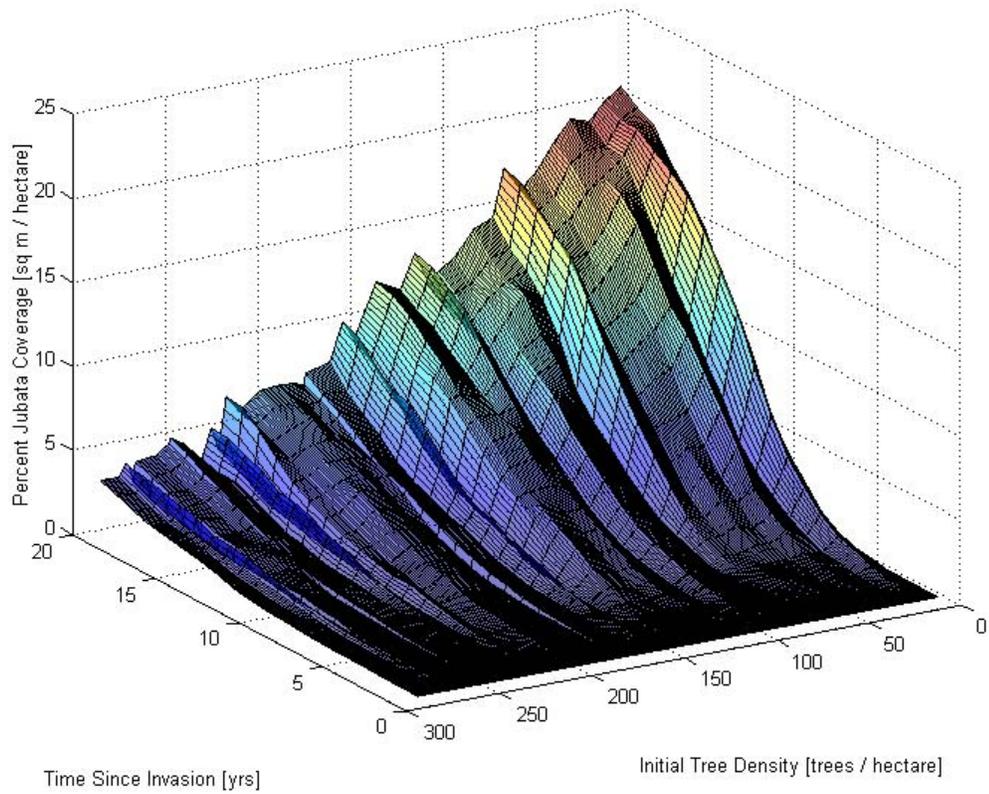
4.   DISCUSSION

In this paper we have created a spatially explicit individual based model to describe the evolution of a landscape as Cortaderia jubata invades a disturbed Sequoia sempervirens forest. The field of neighborhood approach to local competition was employed to describe the contest for all resources in a homogeneous landscape. We found this method acceptable in that it created realistic stand dynamics from local competition. Additionally, we created several methods of visually describing the model's state variables in an effort to not only develop the model, but also to analyze it. The biomass density trajectory description of plant evolution provided a means of identifying the self thinning attributes of plants as well as observing the effects of varying the growth parameters. The landscape animations we created allowed us to watch the forest grow and evolve, which provided a description of plant location and size. To consider plant competition explicitly, we created animated surfaces to describe both total competition for each point in the landscape, as well as the normalized competition experienced per plant, over time. These description were useful, in addition to the landscape animations, in parameterizing the competition strength. The total competition and normalized competition surfaces were particularly useful in parameterizing the seedling and recruitment phases of jubata grass growth, and the memory process respectively. Lastly, we created three visualizations of the percent coverage of the jubata grass. These depictions allowed for a more robust description of the model's output over all initial densities and all time steps.

4.1   Biomass Density Trajectory

We calculated the biomass density trajectories for several values of the field of

neighborhood parameter b. The biomass density trajectory is a visualization of how the

number of trees is related to the average biomass over time. We found the averages of 50

simulations for each value b. This analysis showed us that the shapes of the trajectories

were qualitatively the same. Also, the biomass density trajectory reveals that increasing

b results in trees being able to reach their maximum mean biomass more quickly. The

graph also shows us that the trees are able to tolerate higher densities for larger values of

b. Since the model produced self thinning populations, it serves as a validation of our

model's ability to create realistic competition for resources in addition to a convincing

landscape structure.

4.2   Frames of an Invasion

We used landscape animations to describe plants spatial location and size as they

evolved over time. This visualization provides us with an excellent, tangible description

of what is occurring across the entire landscape, on any given year, and how those

dynamics affect subsequent development. We used the landscape animations extensively

throughout the development of the model to verify that the software was doing what we

intended it to do. Graphs are inherently useful for displaying what would amount to huge

lists of less tractable information. By visualizing the entire landscape we were able to

watch the dynamics of hundreds of plants in different locations at one time. The

landscape views were also relevant in helping describe what other correlated depictions

of model output meant from a visual basis.

4.3   Descriptions of Competition

We generated animated surfaces to describe plant competition for both

competition variables used within the context of this model: F, the total competition for

resources at a location, and F_A, the normalized competition experienced by a single

plant. These descriptions were useful in parameterizing not only competition strength,

but also seed dispersal and recruitment for the jubata species.

The surfaces that describe total competition, F, validated the accurate use of the

field of neighborhood approach by showing heightened competition in those regions in

which more than one plant was competing. These surfaces also showed the characteristic

exponentially decreasing competition strength exerted by individual plants as one moves

away from a plant's center. The frames of the animation we provided for this description

of competition reveal a jubata plant established along an invasion front whose influence

is not yet reaching the trees in the neighboring forest. At year 5 it becomes evident that

the initial jubata plant has grown immensely in the face of limited competition and it now

exerts a much broader field of neighborhood, within which it competes for resources.

Also, the initial invader has succeeded in establishing some offspring within a few gaps

of the forest floor where competition for resources was low. By year 10 the total

competition across the landscape really starts to intensify with larger values of F seen

throughout. More grass has infiltrated remaining areas of the invasion front and the

populations previously established within the forest are now spreading to more remote

areas of low competition. At year 20, any area that was previously vacant from

competition is now being vigorously fought for with even higher values of F in more

locations. This type of heightened competition over a prolonged period of time affects

growth and leads to the possibility of plant death.

It is the normalized competition strength, F_A, that more directly describes the

radial growth and death processes. So, we created animated surfaces to describe F_A for

each individual across the landscape simultaneously over the period of invasion. When

the invasion is initialized, the trees in the forest are experiencing intra-specific

competition, but these values are low enough to allow radial growth, i.e., $F_A < C$. The

influence of the jubata grass does not enter the forest so we see that for our invading

plant, $F_A = 0$. In the next graph, at year 5, the jubata plant along the invasion front is

now visible as it is beginning to experience the slightest amount of competition with a

value of F_A below 0.1. At the same time, competition within the forest is rising slightly

with the establishment of a few more jubata plants. By year 10 we see many plants now

occupy the invasion front, causing a heightened competition to be introduced to this

region. Elsewhere the normalized competition strength is increased by the introduction

of more jubata grass throughout the forest, which creates competition levels that prohibit

growth entirely, those in excess of the threshold C. When the normalized competition

strength has evolved for 20 years, values of F_A are higher than ever since individuals are competing more intensely as the jubata grass has populated the entire landscape.

Both of these descriptions of plant competition, F and F_A, are highly relevant components of the modeling assumptions. Creating graphical descriptions of these values allows us to visualize their spatial and temporal relevance. Further, with these images compiled into an animation, we are able to watch these surfaces change in annual increments. In the case of F, we see undulating waves of total competition strength while in the animation of F_A, we watch cones rise out of the forest floor, with their positions representing plant locations, and their heights representing normalized competition strengths.

4.4   Management Tools

In an effort to exemplify the model's output in a robust and meaningful way, we created images capable of describing the percent coverage of the jubata grass as a function of time and initial tree density. We simulated 100 years of redwood growth for 40 different initial stand densities. We then disturbed 10 percent of each forest along an invasion front in which we introduced a single pampas plant. The plants grew and competed for the next 20 years. The graphical depiction of this information resulted in slices of what could be viewed as a surface. We interpolated across initial densities to create a surface that predicts percent jubata coverage.

This surface reveals more information in a single image than our other descriptions and is thus aptly suited for use in management considerations. It is evident

that the grass is unable to successfully found populations for initial tree densities greater than 200 trees per hectare. For lesser densities, the jubata grass is capable of achieving 5-20% coverage while remaining below 5% for higher densities. The percent coverage surface also reveals interesting qualities of the rate of change of percent coverage by considering the slope along the time axis. We can see that the forest is invaded more quickly with lower density forests exhibiting the increased slopes found along this region of the surface. We also represented the surface with a contour plot that reveals in a simpler, and perhaps more widely accessible way, several phases of jubata grass coverage across a wide range of conditions. These phases are delineated by the contours revealing relative levels of jubata abundance, while still correlating these values with both time and initial redwood densities .

5. CONCLUSION

In summary, the timely establishment of jubata grass is largely suppressed by higher initial densities of trees. Additionally, the rate of jubata expansion is curtailed by these higher densities. Each of the visual descriptions we have presented has merit in that they all reveal different qualities of the model. The percent coverage surface is unique in that it reflects enough information as to appeal to the interests of a forest manager across a range of time scales, tree densities, and levels of existing jubata abundance. Further research could include longitudinal studies to establish larger data sets for estimation of optimal growth curves and other species specific information.

LITERATURE CITED

Abate, Tom 1992. Which bird is the better indicator species for old-growth forest? *BioScience*, 42(1): 8-9.

Allen, G., Lindquist, J., Melo, J., Stuart, J. 1996. Seventy-two years growth on a redwood sample plot: the wonder plot revisited. Proceedings of the conference on coast redwood forest ecology and management. June 18-20, 1996. Arcata, CA. Humboldt State University.

Andow, D.A., Kareiva, P.M., Levin, S.A., & Okubo, A. 1990. Spread of invading organisms. *Landscape Ecology*, 4: 177-188.

Berger, U. and Hildebrandt, H., and Grimm, V. 2002. Towards a standard for the individual-based modeling of plant populations: self-thinning and the field-of-neighborhood approach. *Natural Resource Modeling*, 15(1): 39-54.

Berger, U. and Hildebrandt, H. 2000. A new approach to spatially explicit modeling of forest dynamics: spacing, ageing and neighborhood competition of mangrove trees. *Ecological Modelling*, 132: 287-302.

Boe, K.N. 1975. Natural seedlings and sprouts after regeneration cuttings in old-growth redwood. PSW-111. Berkeley, CA: U.S. Department of Agriculture, Forest Service, Pacific Southwest Forest and Range Experiment Station. 17 p.

Brown, Peter M. 1996. OLDLIST: A database of maximum tree ages. P. 727-731 in Dean, J.S., D.M. Meko and T.W. Swetnam, editors, *Tree Rings, Environment and Humanity*, Proceedings of the International Conference. Radiocarbon 1996, Department of Geosciences, The University of Arizona, Tucson.

Burke, M.J.W. and Grime, J. P. 1996. An experimental study of plant community invisibility. *Ecology*, 77(3): 776-790.

Cooper, D.W. 1967. Pampas grass in Humboldt County. *Agronomic Notes*, June:19-20.

Cowan, B.D. 1976. The menace of pampas grass. *Fremontia*, 4:14-16.

Costas-Lippmann, M. 1976. Ecology and reproductive biology of the genus Cortaderia in California. Ph.D. Thesis, Univ. California, Berkeley. 365 pp.

D'Antonio, C.M. and Vitousek, P.M. 1992. Biological invasions by exotic grasses, the grass/fire cycle, and global change. *Annual Review of Ecology and Systematics*, 23: 63-87.

DiTomaso, J.M., Healy, E., Bell, C.E., Drewitz, J. and Tschohl, A. 1999. Pampas grass and jubata grass threaten California coastal habitats. California Exotic Pest Plant Council, Davis, CA.

Drake, J.A., Mooney, H.A., DiCastri, F., Groves, R.H., Kruger, F.J., Rejmanek, M. and Williamson, M. 1989. *Biological Invasions: A Global Perspective*. John Wiley and Sons, Chichester.

Grimm, V., 1999. Ten years of individual-based modelling in ecology: what have we learned, and what could we learn in the future? *Ecological Modelling*, 115: 129-148.

Grimm, V., 2002. Visual debugging: a way of analyzing, understanding, and communicating bottom-up simulation models in ecology. *Natural Resource Modeling*, 15: 23-38

Higgins, S.I. & Richardson, D.M. 1998a. A review of models of alien plant spread. *Ecological Modelling*, 87: 249-265.

Higgins, S.I. & Richardson, D.M. 1998b. Pine invasions in the southern hemisphere: modeling interactions between organism, environment and disturbance. *Plant Ecol*., 135: 79-93.

Higgins, S.I., Richardson, D.M., and Cowling, R.M. 1996. Modeling invasive plant spread: the role of plant-environment interactions and model structure. *Ecology*,77(7): 2043-2054.

Higgins, S.I., Richardson, D.M., and Cowling, R.M. 2000. Using a dynamic landscape model for planning the management of alien invasions. *Ecological Applications*, 10(6): 1833-1848.

Jenkins, J., Chojnacky, D.C., Heath, L.S., and Birdsey, R.A. 2003. National-scale biomass estimators for United States tree species. *Forest Science*, 49(1): 12-35.

Lambrinos, J.G. 2000. The expansion and impact of alien Cortaderia in California. Ph.D. Thesis, UCLA.

Lambrinos, J.G. 2001. The expansion history of a sexual and asexual species of Cortaderia in California, USA. *Journal of Ecology*, 89: 88-98.

Lambrinos, J.G. 2002. The variable invasive success of Cortaderia species in a complex landscape. *Ecology*, 83: 518-529.

Metcalf, W. 1924. Artificial reproduction of redwood. *Journal of Forestry*, 22: 873-893.

Okubo, A. 1980. *Diffusion and Ecological Problems: Mathematical Models*. Springer-Verlag, Berlin.

Olson, David F., Jr.; Roy, Douglass F.; Walters, Gerald A. 1990. Sequoia sempervirens (D. Don) Endl. redwood. In: Burns, Russell M.; Honkala, Barbara H., technical coordinators. Silvics of North America. Volume 1. Conifers. Agric. Handb. 654. Washington, DC: U.S. Department of Agriculture, Forest Service: 541-551.

Pleasants, A.B. and Whitehead, P.H. 1977. Pampas grass as winter feed. *New Zealand J. Agric*. 135(1): 2-3.

Popay, I., Timmins, S.M., McCluggage, T. 2003. Aerial spraying of pampas grass in difficult conservation sites. *Science for Conservation*, 218. 18p.

Skellam, J.G. 1951. Random dispersal in theoretical populations. *Biometrika* 38: 196-218.

Vitousek, P.M., C.M. D'Antonio, L.L. Loope, and R. Westbrooks. 1996. Biological invasions as global environmental change. *American Scientist*, 84: 468-478.

Watkinson, A.R., Freckleton, R.P., & Forrester, L. 2000. Population dynamics of Vulpia ciliata: regional, patch and local dynamics. *Journal of Ecology*, 88: 1012-1029.

Whipker, B.E., McCall, I., Adkins, C., Sellmer, J. 2007. Control of pampas grass growth with A-Rest, Bonzi and Sumagic Drenches. North Carolina State University Floriculture Report. Referenced on 01 Nov 07 http://www.ces.ncsu.edu/depts/hort/floriculture/hrs/Hrs001.pdf

Wu, J. 1994. Modeling dynamics of patchy landscapes: linking metapopulation theory, landscape ecology and conservation biology. *1993 Yearbook of Dept. of Systems Ecology*. Chinese Academy of Sciences, Beijing.

Wu, J. and Levin, S. 1994. A spatial patch dynamic modeling approach to pattern and process in an annual grassland. *Ecological Monographs*, 64(4): 447-464.